Retrieval of atmospheric CH_4 vertical information from ground-based FTIR near-infrared spectra

Minqiang Zhou[1], Bavo Langerock[1], Mahesh Kumar Sha[1], Nicolas Kumps[1], Christian Hermans[1], Christof Petri[2], Thorsten Warneke[2], Huilin Chen[3], Jean-Marc Metzger[4], Rigel Kivi[5], Pauli Heikkinen[5], Michel Ramonet[6], and Martine De Mazière[1]

[1]Royal Belgian Institute for Space Aeronomy (BIRA-IASB), Brussels, Belgium
[2]Institute of Environmental Physics, University of Bremen, Bremen, Germany
[3]Centre for Isotope Research (CIO), Energy and Sustainability Research Institute Groningen (ESRIG), University of Groningen, Groningen, the Netherlands
[4]UMS 3365 – OSU Réunion, Université de La Réunion, Saint-Denis, Réunion, France
[5]Finnish Meteorological Institute, Space and Earth Observation Centre, Sodankylä, Finland
[6]Laboratoire des Sciences du Climat et de l'Environnement (LSCE/IPSL), UMR CEA-CNRS-UVSQ, Gif-sur-Yvette, France

Correspondence: Minqiang Zhou (minqiang.zhou@aeronomie.be)

Abstract. TCCON (Total Carbon Column Observing Network) column-averaged dry air mole fraction of CH_4 (X_{CH_4}) measurements have been widely used to validate satellite observations and to estimate model simulations. The GGG2014 code is the standard TCCON retrieval software performing a profile scaling retrieval. In order to obtain several vertical information in addition to total column, in this study, the SFIT4 retrieval code is applied to retrieve CH_4 mole fraction vertical profile from the Fourier transform infrared (FTIR) spectrum at six sites (Ny-Ålesund, Sodankylä, Bialystok, Bremen, Orléans and St Denis) during the time period of 2016 – 2017. The retrieval strategy of the CH_4 profile retrieval from ground-based FTIR near-infrared (NIR) spectra using the SFIT4 code (SFIT4NIR) is investigated. The degree of freedom for signal (DOFS) of the SFIT4NIR retrieval is about 2.4, with two distinct pieces of information in the troposphere and in the stratosphere. The averaging kernel and error budget of the SFIT4NIR retrieval are presented. The data accuracy and precision of the SFIT4NIR retrievals, including the total column and two partial columns (in the troposphere and stratosphere), are estimated by TCCON standard retrievals, ground-based in situ measurements, ACE-FTS satellite observations, TCCON proxy data, AirCore and aircraft measurements. By comparison against TCCON standard retrievals, it is found that the retrieval uncertainty of SFIT4NIR X_{CH_4} is similar to that of TCCON standard retrievals with the systematic uncertainty within 0.35% and the random uncertainty about 0.5%. The tropospheric and stratospheric X_{CH_4} from SFIT4NIR retrievals are assessed by comparing with AirCore and aircraft measurements, and there is a $1.0 \pm 0.3\%$ overestimation in the SFIT4NIR tropospheric X_{CH_4} and a $4.0 \pm 2.0\%$ underestimation in the SFIT4NIR stratospheric X_{CH_4}, which are within the systematic uncertainties of SFIT4NIR retrieved partial columns in the troposphere and stratosphere, respectively.

1

1 Introduction

The Total Carbon Column Observing Network (TCCON) is an international network established in 2004 using ground-based Fourier transform infrared (FTIR) spectrometers to record direct solar absorption spectra in the near-infrared (NIR) spectral range and to retrieve from these spectra total columns of atmospheric greenhouse gases, including methane (CH_4) (Wunch et al., 2011). Currently, there are about 25 TCCON sites around the world with a latitude coverage from 45°S to 80°N. The standard TCCON retrieval code is GGG2014 (developed and maintained at JPL, NASA); it performs a profile scaling retrieval. TCCON provides the dry air total column averaged mole fraction of CH_4 (X_{CH_4}), which have been compared to and indirectly calibrated by the Infrastructure for the Measurement of the Europe Carbon Cycle (IMECC) profiles over the European TCCON stations, the high-performance instrumented airborne platform for environmental research (HIAPER) Pole-to-Pole Observations (HIPPO) profiles over the TCCON stations in Northern America East Asia and Oceania, and several AirCore profiles (Karion et al., 2010) over Lamont (USA). A scaling factor of 0.977±0.002 (1σ) is applied to the retrieved X_{CH_4} values to correct for the systematic bias. As one fixed value of 0.977 is applied to all the TCCON sites, the site-to-site bias is not taken into account. It is assumed that the remaining systematic uncertainty of the TCCON X_{CH_4} products is within 0.2%. The random uncertainty of the X_{CH_4} retrieval is about 0.5% (Wunch et al., 2015). TCCON X_{CH_4} observations have relatively larger footprints compared to surface in situ measurements, and thus could provide flux information on a regional scale (Wunch et al., 2016). TCCON X_{CH_4} measurements are widely used to validate the satellite observations, e.g. the Scanning Imaging Absorption Spectrometer for Atmospheric Chartography (SCIAMACHY) and the Thermal And Near-infrared Sensor for carbon Observation Fourier-Transform Spectrometer (TANSO-FTS) (Houweling et al., 2014; Dils et al., 2014; Zhou et al., 2016). In addition, the TCCON X_{CH_4} observations are also used to evaluate atmosphere chemistry transport model simulations (Saito et al., 2012; Fraser et al., 2013; Agusti-Panareda et al., 2017).

The concentration of atmospheric CH_4 remained almost constant from about 1995 to 2006. However, after 2007, the CH_4 concentration started to increase with an annual growth rate about 0.7 ppb/year (Rigby et al., 2008). The CH_4 in the atmosphere is released from gas and oil, coal, landfill, ruminant animal, rice agriculture, biomass burning, wetland and lake. The CH_4 in the troposphere is removed mainly by the oxidation with hydroxyl radicals (OH), partly by getting absorbed in the soil and party by reacting with chlorine radicals in the marine boundary layer. The CH_4 in the stratosphere is removed by the oxidation with OH, chlorine atoms and excited oxygen atoms (IPCC, 2013). The mole fraction of CH_4 decreases rapidly with altitude above the tropopause due to a higher photolysis rate in the stratosphere (Ehhalt and Heidt, 1973). The separation of the tropospheric and stratospheric CH_4 partial columns helps to better understand the atmospheric CH_4 variability and to comprehensively evaluate model simulations (Ostler et al., 2016; Saad et al., 2016; Wang et al., 2017). The seasonal variation of CH_4 in the troposphere is dominated by its source and sink as well as the horizontal transport, while seasonal variation of CH_4 in the stratosphere is strongly affected by the Brewer-Dobson circulation, the vertical transport, the intertropical convergence zone movement and stratospheric chemical reactions. A proxy method to derive the tropospheric and stratospheric X_{CH_4} from the TCCON retrievals based on the known relationship between CH_4 and hydrogen fluoride (HF) or nitrous oxide (N_2O) in the stratosphere has already been demonstrated by Wang et al. (2014) and Saad et al. (2014). The N_2O and HF total columns are

also available in the TCCON standard products. An alternative CH_4 profile retrieval method has been provided by Tukiainen et al. (2016), using dimension reduction and the Markov chain Monte Carlo statistical estimation.

In this study, the CH_4 profile retrieval from ground-based FTIR near-infrared spectra using the SFIT4 code (named SFIT4NIR retrievals) is carried out at six sites (Ny-Ålesund, Sodankylä, Bialystok, Bremen, Orléans and St Denis) for measurements performed during the time period of 2016-2017 in the framework of the EU Readiness of ICOS for Necessities of integrated Global Observations (RINGO) project. The full-physics SFIT4 retrieval code is based on the optimal estimation method (Rodgers, 2000), which is an updated version of SFIT2 (Pougatchev et al., 1995) and commonly used in the Network for the Detection of Atmospheric Composition Change - the Infrared Working Group (NDACC-IRWG) (De Mazière et al., 2018). The TCCON sites and the SFIT4NIR retrieval strategy are introduced in the next section. The motivation behind this study is to retrieve vertical information of CH_4 from TCCON spectra. In section 3 the difference in X_{CH_4} retrieved using the SFIT4NIR to the X_{CH_4} retrieved from the standard TCCON retrievals is investigated. The tropospheric and the stratospheric X_{CH_4} retrieved using the SFIT4NIR retrievals are compared with other available datasets, such as ground-based in situ measurements, Atmospheric Chemistry Experiment - Fourier Transform Spectrometer (ACE-FTS) satellite observations, and TCCON proxy data. Furthermore, the comparison results from the SFIT4NIR retrievals relative to the AirCore and aircraft profiles are also discussed in this section. Finally, conclusions are drawn in Section 4.

2 Data and method

2.1 TCCON sites

The locations of the TCCON sites used in this study are listed in Table 1. All sites use a Bruker IFS 125HR instrument to record NIR spectra in the range of 5000-10000 cm^{-1} with a spectral resolution of 0.02 cm^{-1}. The TCCON spectra from all sites in the time period of 2016-2017 were transferred to BIRA-IASB. A DC correction is applied to remove the variation of the interferogram caused by the solar intensity variation due to the presence of clouds during a measurement (Keppel-Aleks et al., 2007). A python code is developed to convert the TCCON spectra from the OPUS format to the SFIT4 readable format.

Table 1. The coordinates and the altitudes (m a.s.l.) of the TCCON FTIR sites used in this study.

Site	Latitude	Longitude	Altitude (m a.s.l.)	Reference
Ny-Ålesund	78.9°N	11.9°E	20	Notholt et al. (2017)
Sodankylä	67.4°N	26.6°E	188	Kivi et al. (2014)
Bialystok	53.2°N	23.0°E	180	Deutscher et al. (2014)
Bremen	53.1°N	8.8°E	30	Notholt et al. (2014)
Orléans	48.0°N	2.1°E	130	Warneke et al. (2014)
St Denis (Reunion Island)	21.0°S	55.4°E	87	De Mazière et al. (2014)

2.2 SFIT4NIR retrieval strategy

The SFIT4NIR retrieval strategy is investigated based on the TCCON spectra at St Denis (a humid site) using the SFIT4_v9.4.4 retrieval code. After that, the optimized retrieval strategy is applied for other sites. The key parameters used in the SFIT4NIR retrieval are listed in Table 2. The atmospheric line list (ATM) used in the GGG2014 code (Toon, 2014) has also been used in the forward model of the SFIT4NIR. A linear polynomial fitting is applied to a time-domain ideal instrument line shape (ILS) and the parameters are retrieved simultaneously. The a priori ILS is set as the ideal ILS. Since the Bruker 125HR spectrometers exhibit excellent ILS stability, the retrieved ILS are very constant and the retrieved maximal variations for modulation efficiency (ME) amplitude are within 2% at these six sites. A detailed description of the retrieval settings, the averaging kernel and the retrieval uncertainty are presented in section 2.2.1 - 2.2.5.

Table 2. Lists of the most important parameters in the SFIT4NIR retrieval strategy.

|	
Retrieval window (cm^{-1})	5996.45-6007.55
Interfering species	CO_2, H_2O
Spectroscopy	ATM
Regularization	Tikhonov L_1 with $\alpha = 1000$
A priori profile	WACCM v6 (fixed)
SNR	250
ILS	a linear polynomial fitting

2.2.1 Retrieval window

Three windows listed in Table 3 are used to retrieve CH_4 total column values using the GGG2014 code. All these retrieval windows were tested with SFIT4NIR retrieval. The typical transmittance and residual for the three windows are shown in Figure 1. The root-mean-square (RMS) of the residual in band 1 is largest due to a bad fitting of several strong H_2O absorption lines. The RMS of the residual in band 2 is the lowest and is slightly better than that in band 3. As an example, the retrieved CH_4 total columns using these three bands on 30 July 2016 are shown in Figure 2. A clearly artificial symmetric variation for band 1 is seen, which is probably due to a bad fitting of the spectra. The results from Band 2 and 3 are similar. The difference between the retrieved CH_4 total columns from Band 2 and 3 are within $0.3 \pm 0.1\%$. As the band 2 has the best fitting, it is selected as the retrieval window for our SFIT4NIR retrieval.

2.2.2 A priori profile

According to the optimal estimation method (OEM) (Rodgers, 2000), a priori profile is used to initialize the iteration during a retrieval process. In this study, SFIT4NIR uses the mean of the monthly profiles between 1980 and 2020 from the Whole Atmosphere Community Climate Model (WACCM) version 6 as the a priori profiles for CH_4 and CO_2, while H_2O a priori profile is derived from the 6-hourly NCEP reanalysis data because of its high variability in the atmosphere.

Table 3. The retrieval windows used in the GGG2014 code.

	Window (cm^{-1})	Width (cm^{-1})	Interfering spices
band 1	5781.0-5897.0	116.0	CO_2, H_2O, N_2O
band 2	5996.45-6007.55	11.1	CO_2, H_2O
band 3	6007.0-6145.0	138.0	CO_2, H_2O
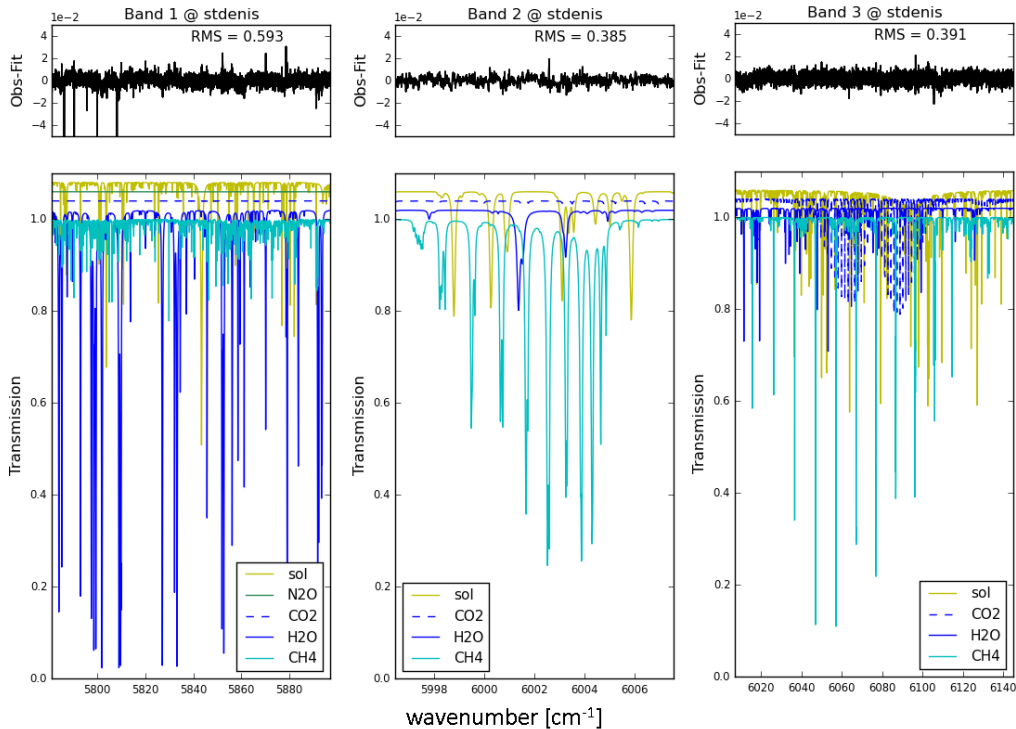
Figure 1. The transmittances of the species and solar lines in three bands from a typical spectrum at St Denis, together with the residual (observation - fitting). The transmittance of each component is shifted by 0.02 to better identify different species and the solar lines (sol).
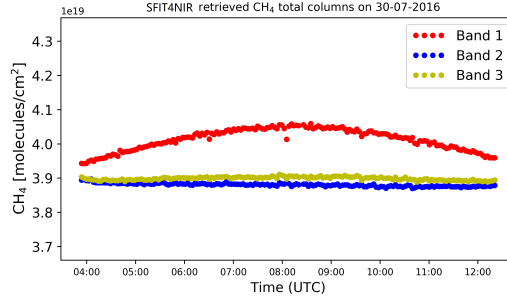
2.2.3 Regularization

The retrieved CH$_4$ profile can be written as

$$x_{r,CH_4} = x_{a,CH_4} + \mathbf{A}(x_{t,CH_4} - x_{a,CH_4}) + \varepsilon, \tag{1}$$

$$\mathbf{A} = (\mathbf{K}^T \mathbf{S}_\varepsilon^{-1} \mathbf{K} + \mathbf{S_a}^{-1})^{-1} \mathbf{K}^T \mathbf{S}_\varepsilon^{-1} \mathbf{K}, \tag{2}$$

where x_{a,CH_4}, x_{t,CH_4} and x_{r,CH_4} are the a priori, true and retrieved CH$_4$ mole fraction profiles, respectively. $\mathbf{A}$ is the averaging kernel, representing the sensitivity of the retrieved CH$_4$ profile to the true atmosphere status. The trace of $\mathbf{A}$ is the

Figure 2. The SFIT4 retrieved CH_4 total columns using the 3 bands listed in Table 1 on 30 July 2016 (184 spectra).

degree of freedom for signal (DOFS), indicating the number of individual vertical information derived from the retrieval. $\mathbf{K}$ is the Jacobian matrix. ε is the retrieval uncertainty. $\mathbf{S_a}$ and $\mathbf{S_\varepsilon}$ are the a priori covariance matrix and the measurement covariance matrix, respectively. $\mathbf{S_\varepsilon}$ is determined by the signal to noise ratio (SNR). $\mathbf{S_a}^{-1}$ and $\mathbf{S_\varepsilon}^{-1}$ are the two key parameters to constrain the retrieved CH_4, and to determine whether the retrieved CH_4 profile is mainly from the a priori information or from the measurement information. It is assumed that $\mathbf{S_\varepsilon}$ is a diagonal matrix, where the diagonal elements are the inverse square of the SNR. The SNR of spectra is set to 250 at all the TCCON sites. $\mathbf{S_a}^{-1}$ is created by the Tikhonov $\mathbf{L}_1$ method (Tikhonov, 1963)

$$\mathbf{S_a}^{-1} = \alpha \mathbf{L}_1^T \mathbf{T} \mathbf{L}_1 \in \mathbf{R}^{(n,n)}, \tag{3}$$

where $L_1 = \begin{bmatrix} -1 & 1 & 0 & \ldots & 0 & 0 \\ 0 & -1 & 1 & \ldots & 0 & 0 \\ \vdots & \vdots & \vdots & \ddots & \vdots & \vdots \\ 0 & 0 & 0 & \ldots & -1 & 1 \end{bmatrix}$, $\mathbf{T} = diag(\Delta h^2)$ (Δh is the thickness of each layer), and regularization strength α is the key parameter to determine the correlation strength among layers.

The optimized α value is chosen by extracting maximum possible information from the measurement while eliminating the artificial oscillation for the retrieved CH_4 profiles. Several α values are tested using the spectra on 30 July 2016, and the RMS, DOFS and retrieved CH_4 total columns are listed in Table 4, along with the retrieved CH_4 vertical profiles in Figure 3. The retrieved CH_4 profile shows a strong oscillation in the troposphere for $\alpha = 100$. The vertical profiles are similar for $\alpha = 1000$ and $\alpha = 10000$, but it allows us to get a smaller RMS with $\alpha = 1000$. In summary, a regularization strength (α) of 1000 with the DOFS of about 2.4 is the selected as the best choice for the SFIT4NIR retrieval.

2.2.4 Averaging kernel

Left panel in Figure 4 shows the typical averaging kernel (AVK) of SFIT4NIR retrieval with a solar zenith angle (SZA) of $63°$ at St Denis. The retrieved CH_4 profile is sensitive to the altitude range from the surface to the middle stratosphere (about

6

Table 4. The mean and standard deviation of RMS, DOFS and retrieved CH_4 total columns from SFIT4NIR retrievals using different regularization strength α values.

| α	100	1000	10000
RMS (%)	0.34±0.06	0.34±0.06	0.35±0.06
DOFS	3.25±0.11	2.42±0.08	1.77±0.04
Total column CH_4 (10^{18} molec/cm^2)	38.62±0.05	38.64±0.04	38.65±0.04
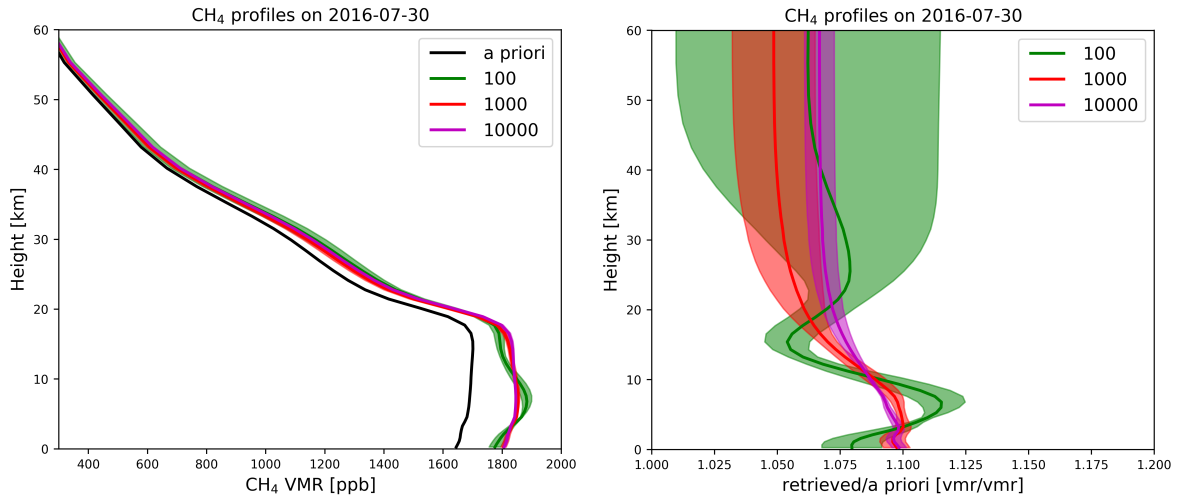
Figure 3. The SFIT4NIR a priori and the retrieved CH_4 vertical profiles (left panel), together with the ratios of the retrieved profiles to the a priori profile (right panel), with different regularization strength α values.

40 km). The AVK shows that the SFIT4NIR retrieved profile contains independent information in the troposphere and in the stratosphere (DOFS close to 1.0 for these two layers). In addition, the column averaging kernels (right panel in Figure 4) indicate that the retrieved CH_4 total column has a good sensitivity in the whole atmosphere, with the value close to 1.0 at all altitudes. The column averaging kernels slightly vary with the SZAs, which is more constant than the AVK variability for the SZAs of the standard TCCON products (see Figure 4 in Wunch et al. (2011)).

2.2.5 Error budget

According to the OEM (Rodgers, 2000), the measurement uncertainty of SFIT4NIR retrieval (ε in Eq. 1) is estimated from three components: the smoothing error covariance matrix ($\mathbf{S}_s$), the forward model parameter error covariance matrix ($\mathbf{S}_f$) and
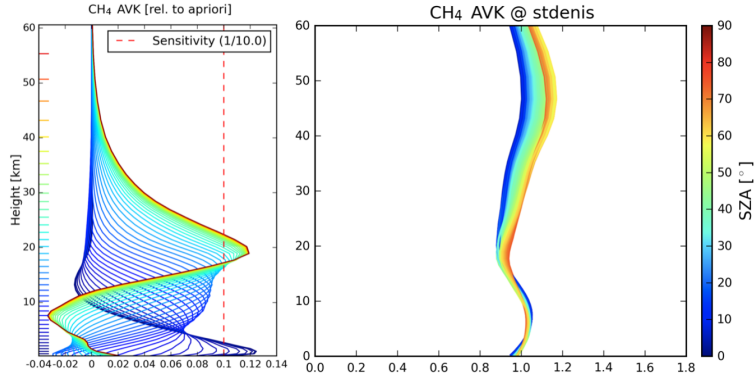
Figure 4. Left panel: a typical CH_4 averaging kernel matrix of the SFIT4NIR retrieval with the SZA of $63°$ at St Denis, in unit of the mole fraction profile with respect to the a priori. Right panel: CH_4 column averaging kernels for different solar zenith angles.

the measurement error covariance matrix ($\mathbf{S}_m$).

$$\mathbf{S}_s = (\mathbf{A} - \mathbf{I})\mathbf{S}_e(\mathbf{A} - \mathbf{I})^T, \tag{4}$$

$$\mathbf{S}_f = \mathbf{G}_y\mathbf{K}_b\mathbf{S}_b\mathbf{K}_b^T\mathbf{G}_y^T, \tag{5}$$

$$\mathbf{S}_m = \mathbf{G}_y\mathbf{S}_\varepsilon\mathbf{G}_y^T, \tag{6}$$

5 where $\mathbf{G}_y$ is the contribution matrix, representing the sensitivity of the retrieval to the measurement. $\mathbf{S}_e$, $\mathbf{S}_b$ and $\mathbf{S}_\varepsilon$ are the covariance matrices of the retrieval state vector, the forward model parameter and the measurement, respectively. The retrieval state vector (x in Eq. 1) not only includes the CH_4 vertical profile, but also includes the H_2O and CO_2 columns, the slope of the background, the wavenumber shift and several ILS parameters. Each retrieved parameter has systematic and random uncertainties. The relative standard deviation of the CH_4 monthly means from the WACCM model in 1980-2020 is calculated

10 as the random uncertainty of the CH_4 profile. For the systematic uncertainty, we have chosen a value of 5% (about 90 ppb in the troposphere), based on the difference between the a priori CH_4 mole fraction near the surface and the local in situ measurements (Zhou et al., 2018). As CH_4 is relatively stable in the atmosphere with a life time of ~ 9 years, it is assumed that 5% systematic uncertainty is acceptable for all altitudes. The systematic and the random uncertainties for H_2O and CO_2 are set to 5%. The systematic and random uncertainties of ILS parameters are set to 1%. The other retrieved parameters do

15 not contribute significantly to the CH_4 uncertainty. The smoothing error in Table 5 represents the uncertainty contribution from the CH_4 vertical profile, while the errors from the retrieved parameters in the Table 5 include the contribution from the H_2O and CO_2 columns, the slope of the background, the wavenumber shift and several ILS parameters. The spectroscopy, the temperature and the SZA are the most important parameters contributing to the forward model. According to the HITRAN2012 (Rothman et al., 2013), the uncertainty of CH_4 absorption in the selected retrieval window is about 2-5%. Therefore, the

20 systematic uncertainty of the spectroscopy is set to 3%, and the random uncertainty on the spectroscopic data is assumed to be negligible. The systematic and random uncertainties are set to 1% for the temperature. The systematic uncertainty is set

8

Table 5. The systematic and random uncertainties for the SFIT4NIR retrieved CH$_4$ total column, partial columns in the troposphere (0–16.5 km) and in the stratosphere (16.5–50 km). The uncertainties are in the unit of percentage (%). The blank place is where the uncertainty is negligible with a value which is less than 0.1%.

Error	Total column		Troposphere (0-16.5 km)		Stratosphere (16.5-50 km)	
	Systematic	Random	Systematic	Random	Systematic	Random
Smoothing	0.2	0.2	0.2	0.2	1.2	1.6
Measurement		0.1		0.1		0.9
Retrieved parameters	0.2	0.2	0.1	0.1	2.5	2.5
Temperature	1.1	0.4	1.0	0.4	1.8	0.5
Spectroscopy	3.1		3.1		6.0	
SZA	0.1	0.2	0.1	0.2	0.2	0.9
Total	3.2	0.5	3.1	0.5	6.8	3.3

to 0.1% and the random uncertainty is set to 0.5% for the SZA. $\mathbf{S}_\varepsilon$ is assumed to be diagonal where the diagonal elements are the inverse square of the SNR. The propagated uncertainties of the total column and the partial columns (troposphere and stratosphere) are listed in Table 5. The mean tropopause height above St Denis is about 16.5 km. The systematic and random uncertainties of the SFIT4NIR retrieved CH$_4$ total column are 3.2% and 0.5%, respectively. The dominating component of the systematic uncertainty is coming from the spectroscopy. The uncertainties of the partial column in the troposphere are closer to those of the total column, while the uncertainties of the partial column in the stratosphere are relatively large.

3 Results and discussions

The retrieval strategy listed in Table 2 is applied for all six sites. In this section, the data quality of the SFIT4NIR retrievals is evaluated with TCCON standard retrievals, ground-based in situ measurements, ACE-FTS satellite remote sensing observations, TCCON proxy X_{CH_4} data and AirCore measurements.

3.1 TCCON standard retrievals

According to Section 2.2.5, the random uncertainty of SFIT4NIR total column is about 0.5%, which is close to that of TCCON retrieval (Wunch et al., 2015). The systematic uncertainty of SFIT4NIR total column is about 3.2% where a large contribution is from the spectroscopy. To better understand the systematic uncertainty of the SFIT4NIR retrieved total column, the SFIT4NIR X_{CH_4} at six sites in 2016-2017 are calculated and compared with TCCON standard products. The systematic uncertainty of TCCON X_{CH_4} products is within 0.2%.

GGG2014 uses the ratio between CH_4 and O_2 total columns to calculate the X_{CH_4} (Yang et al., 2002), as the atmospheric O_2 mole fraction is relatively stable with the mole fraction of 0.2095

$$X_{CH_4} = 0.2095\, TC_{CH_4}/TC_{O_2}. \tag{7}$$

The X_{CH_4} from the SFIT4NIR retrieval is calculated as

$$X_{CH_4} = \frac{TC_{CH_4}}{TC_{air}^{dry}} = \frac{TC_{CH_4}}{P_s/(gm_{air}^{dry}) - TC_{H_2O}(m_{H_2O}/m_{air}^{dry})}, \tag{8}$$

where TC_{air}^{dry} and TC_{H_2O} are total columns of dry air and H_2O; P_s is the surface pressure; g is the total column-averaged gravitational acceleration; m_{H_2O} and m_{air}^{dry} are molecular masses of H_2O and dry air, respectively (Deutscher et al., 2010). The uncertainty of P_s is better than 0.1 hPa and the uncertainty of H_2O column in the troposphere is about 5-10%, as a result, the uncertainty of the dry air column is about 0.1%. The uncertainty of X_{CH_4} is the combination of the uncertainties of the total column of CH_4 and the dry air column, while the uncertainty of the dry air column is negligible compared to the uncertainty of SFIT4NIR retrieval (see Table 5). The SFIT4NIR tropospheric and stratospheric X_{CH_4} can be calculated following Eq. 8 using the partial columns of CH_4 and dry air in the troposphere and in the stratosphere, respectively. The tropopause height is calculated individually for each SFIT4NIR retrieval using the temperature and pressure profiles from the NCEP 6-hourly reanalysis data. The tropopause height varies from site-to-site according to its latitude. The tropopause height is about 8–11 km at Ny-Ålesund and Sodankylä, 10–12 km at Bialystok, Bremen and Orléans, and 16–17 km at St Denis.

Figure 5 shows the time series of the hourly means of X_{CH_4} from SFIT4NIR and TCCON retrievals and their differences for measurements performed in 2016-2017. The mean and standard deviation of the X_{CH_4} difference between SFIT4NIR and TCCON (SFIT4NIR - TCCON) at the six sites are in the range between -2.3 ppb (-0.14%) and 2.5 ppb (0.15%) and between 4.7 ppb (0.3%) and 9.9 ppb (0.5%). The standard deviations of the differences at all sites are within 0.5%, which is consistent with the combined random uncertainties from SFIT4NIR and TCCON retrievals. The systematic bias between the SFIT4NIR and TCCON retrieved X_{CH_4} is much lower than 3.2%, indicating that the systematic uncertainty of SFIT4NIR total column from the spectroscopy (see Table 3) is overestimated. Since the systematic uncertainty of TCCON X_{CH_4} retrieval is better than 0.2%, it is inferred that the systematic uncertainty of SFIT4NIR X_{CH_4} retrieval is within 0.35%. Figure 6 shows the scatter plots of the X_{CH_4} retrievals from SFIT4NIR and TCCON at the six sites. The linear regression line (dashed red line) is very close to the one-to-one lines for all panels. The correlation coefficient is in the range between 0.76 and 0.94. No obvious seasonal variation is seen from Figure 5 and 6.

3.2 In situ measurements

This section presents the comparison results between the ground-based in situ measurements at the individual sites and the tropospheric X_{CH_4} retrieved using SFIT4NIR. Ground-based in situ measurements are more sensitive to the local sources and sinks as compared to the FTIR measurements. The Traînou tower at Orléans site operates in situ measurements at four heights (180, 100, 50 and 5 m). The measurements at 180 m are used here as they are less affected by the boundary layer (Schmidt et al., 2014). In situ measurements for the St Denis site are taken from the measurements performed at Maïdo (2155 m) located
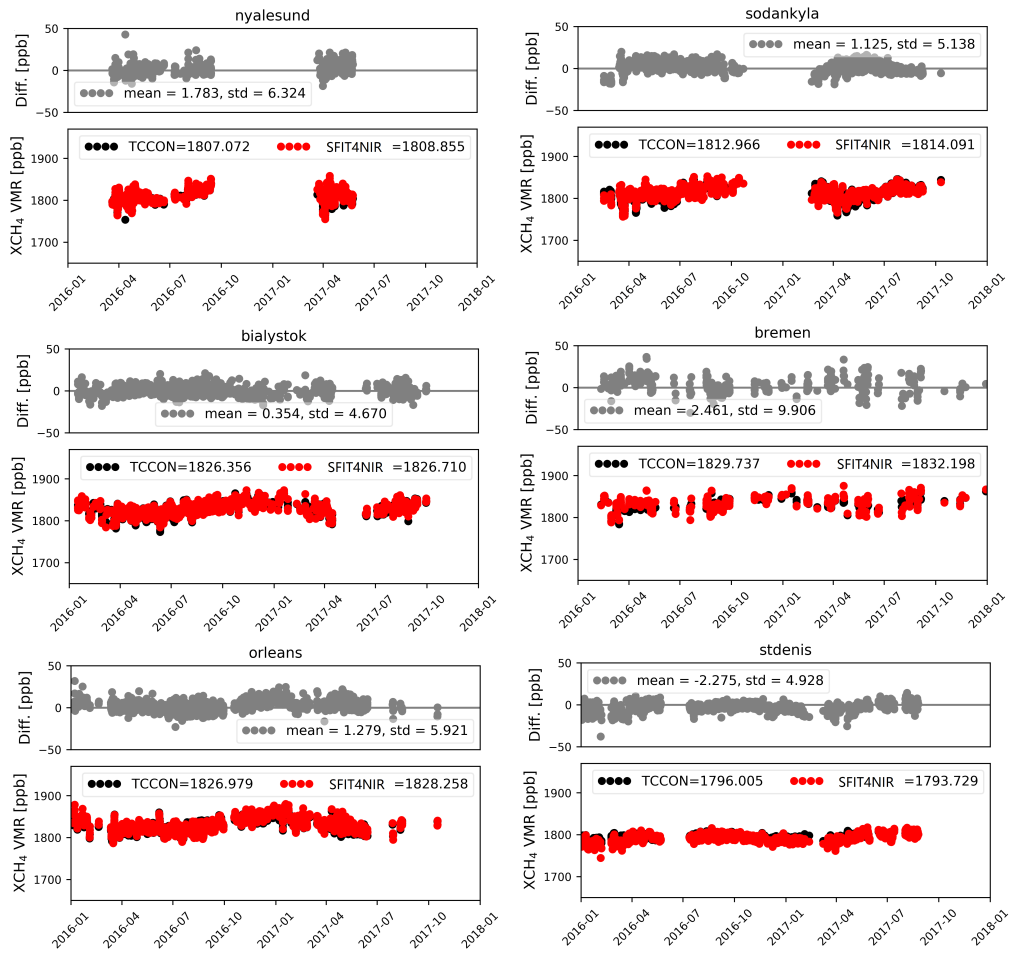
Figure 5. The time series of hourly means of X_{CH_4} from the SFIT4NIR and the TCCON retrievals at six TCCON sites during 2016 – 2017, together with their differences. For each site, the lower panel shows the time series of SFIT4NIR and TCCON measurements, and the upper panel shows the absolute difference between them (SFIT4NIR - TCCON; in ppb units). The values in the legend of the lower panel are the means of the TCCON and SFIT4NIR retrievals.

at about 20 km away from St Denis (Zhou et al., 2018). The in situ measurements at Maido are less affected by the surface, and CH_4 is well-mixed in the lower atmosphere with a life time of 8-10 years (Kirschke et al., 2013). Both ground-based in situ measurements at Orléans and Maïdo are calibrated frequently at the Laboratoire des Sciences du Climat et de l'Environnement (LSCE). The in situ measurements from other sites are not used in order to reduce the influence from the boundary layer.

5   Figure 7 shows the monthly means and standard deviations of the co-located ground-based in situ and the SFIT4NIR tropospheric X_{CH_4} hourly means at Orléans and St Denis in 2016. In general, the seasonal cycle from the in situ measurements is similar to the one from the SFIT4NIR tropospheric X_{CH_4} retrievals at these two sites. However, the in situ tower measurements (180 m) at Orléans are still influenced by the boundary layer, and several high spikes are observed in March, June and Decem-

11
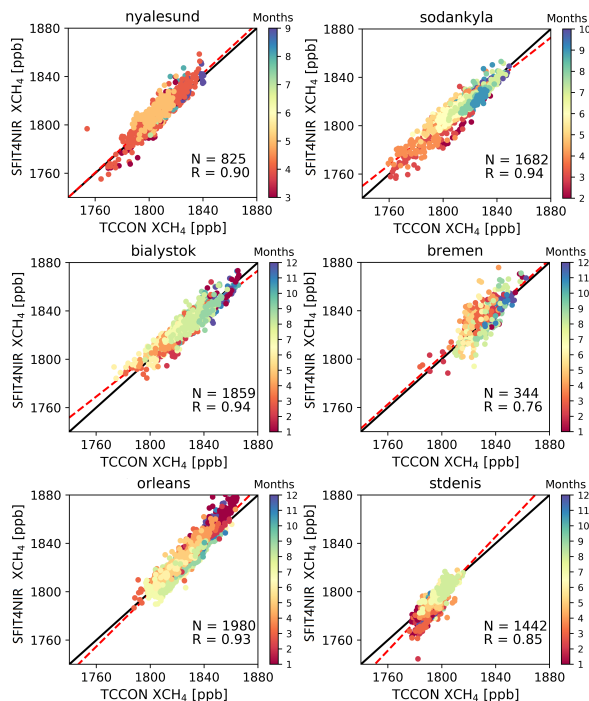
Figure 6. The scatter plots between SFIT4NIR and TCCON X_{CH_4} hourly retrievals at the six TCCON sites. The dots are colored with the measurement months. In each panel, the black line is the one-to-one line and the dashed red line is the linear fitting. N is the measurement number, and R is the correlation coefficient.
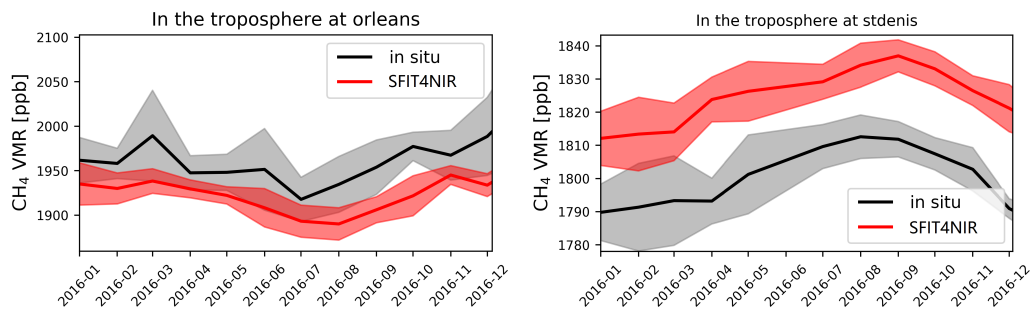
Figure 7. The time series of the monthly means (solid line) and standard deviations (shadow) from the SFIT4NIR tropospheric X_{CH_4} and the ground-based in situ CH_4 measurements at Orléans (left panels) and at St Denis (right panels). At Orléans, the in situ measurements are recorded at 180 m on a tower at the same place. The in situ measurements at St Denis are recorded at 2155 m on the Maïdo mountain, which is about 20 km away from St Denis.

ber 2016. The in situ measurements at Orléans are found to be about 36 ppb larger than the SFIT4NIR tropospheric X_{CH_4}. Schmidt et al. (2014) showed that the CH_4 mole fractions at the 4 layers of the Orléans tower measurements are decreasing

with increasing altitude. There is a strong CH_4 anthropogenic emission around Orléans (European Commission, 2013), which remains mainly at the surface. This might explain the bias between the SFIT4NIR tropospheric X_{CH_4} and the in situ tower measurements at Orléans. The in situ measurements at St Denis are found to be about 24 ppb lower than the SFIT4NIR tropospheric X_{CH_4}. Zhou et al. (2018) pointed out that the air near the surface above St Denis (0-2 km) is mainly coming from the Indian Ocean and partly from Southern African region, whereas the air mass in the middle and upper troposphere (4-12 km) is mainly coming from Africa and South America. As CH_4 emission on the land is much larger than that from the ocean, it is reasonable that SFIT4NIR tropospheric X_{CH_4} is systematically larger than the CH_4 mole faction at the surface.

The phases and amplitudes of the seasonal cycles from the SFIT4NIR tropospheric X_{CH_4} and the ground-based in situ CH_4 measurements are found to be in good agreement. CH_4 mole fraction is high in December – March and low in July – September at Orléans (located in Northern Hemisphere), and high in July – September and low in December – March at St Denis (located in Southern Hemisphere). The CH_4 seasonal variations in the troposphere are driven by the OH variation, which is the major sink of CH_4 in the atmosphere.

3.3 ACE-FTS satellite observations

The comparison results between the SFIT4NIR stratospheric X_{CH_4} and the ACE-FTS satellite observations are discussed in this section. The vertical range from the tropopause height up to 50 km is treated as the stratosphere in this study. ACE-FTS satellite monitors the atmospheric CH_4 concentration mainly in the stratosphere since 2004 in the solar occultation mode (Bernath et al., 2005). The latest level 2 version 3.6 data with data quality flag equal to 0 (without any known issue) are selected from ACE/SCISAT dataset (Sheese et al., 2015). The ACE-FTS CH_4 profile is retrieved on target altitudes with a vertical resolution of 3-4 km, and then it is interpolated onto a 1 km grid. The older version v2.2 data of the ACE-FTS CH_4 data have been compared to space-based satellite, balloon-borne and ground-based FTIR data (De Maziere et al., 2008). The accuracy of the version 2.2 data is within 10% in the upper troposphere - lower stratosphere, and within 25% in the middle and higher stratosphere up to the lower mesosphere. The uncertainty of the new version of the ACE-FTS data has a reduction of about 10% near 35-40 km and a slight reduction at 23 km (Waymark et al., 2014).

Figure 8 shows the SFIT4NIR and ACE-FTS co-located daily means of the stratospheric X_{CH_4} at Bialystok, Orléans and St Denis. The ACE-FTS measurements are selected within $\pm 3 \times 30°$ (latitude by longitude) around each FTIR site. Limited co-locations are found for Ny-Ålesund, Sodankylä and Bremen sites and so the results are not shown here. Figure 8 shows that the seasonal cycles (both phase and amplitude) of the stratospheric X_{CH_4} from SFIT4NIR and ACE-FTS are similar. The stratospheric X_{CH_4} shows a minimum in February-April and a maximum in August-October for the Bialystok and Orléans sites located in the northern hemisphere. Whereas, the stratospheric X_{CH_4} shows a minimum in August-October and a maximum in February-April for St Denis site located in the southern hemisphere. The mean and the standard deviation of the differences in stratospheric X_{CH_4} between the SFIT4NIR and ACE-FTS measurements at these three sites are in the range between -0.27 and 2.06% and between 1.92 and 3.21%, respectively, which are within their uncertainties.
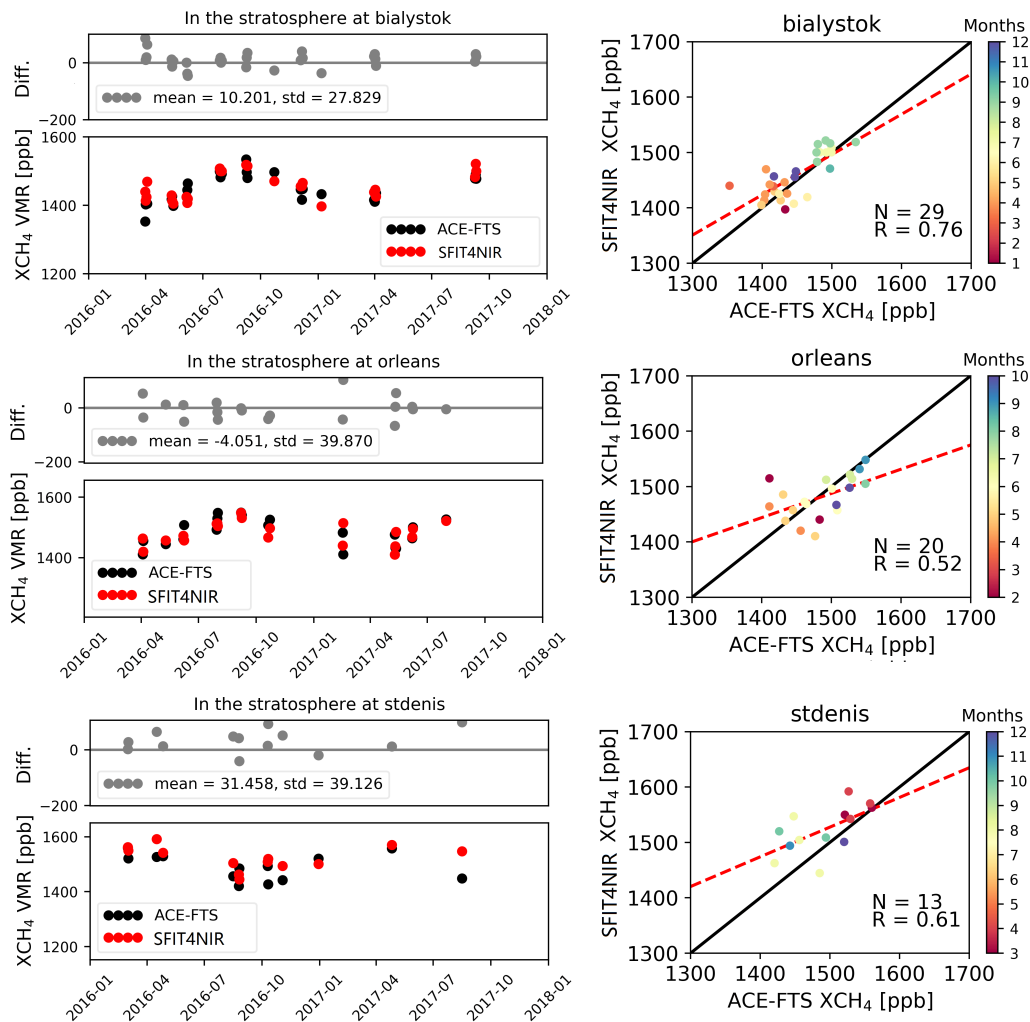
Figure 8. Left panels: the time series of the daily mean of the stratospheric X_{CH_4} from the SFIT4NIR and the ACE-FTS co-located daily mean measurements, together with the absolute difference (unit: ppb) between them for Bialystok, Orléans and St Denis. Right panels: the correlation plots between the SFIT4NIR and the ACE-FTS co-located stratospheric X_{CH_4} daily means.

3.4 TCCON proxy data

In this section, the tropospheric and stratospheric X_{CH_4} from SFIT4NIR retrievals are compared with the results derived from the N_2O and HF proxy methods at the six TCCON sites. We refer to Wang et al. (2014) and Saad et al. (2014) for the details of computing the tropospheric and stratospheric X_{CH_4} by the proxy retrieval method using N_2O and HF. Figure 9 shows the time

5   series of the tropospheric and stratospheric X_{CH_4} from the TCCON proxy N_2O and HF method. First, the tropospheric and stratospheric X_{CH_4} from the N_2O and HF proxy methods are close to each other. However, a slight seasonal and site dependent

bias is observed. For example, the difference in tropospheric X_{CH_4} between N$_2$O proxy method and HF proxy method is larger in summer than that in winter at Ny-Ålesund. The tropospheric X_{CH_4} from N$_2$O and HF proxy method are very close to each other for St Denis. While for the other five sites, the tropospheric X_{CH_4} from the N$_2$O method is larger by about 15-20 ppb than the HF method. The bias in the tropospheric X_{CH_4} between the N$_2$O and HF methods are in a good agreement with the

5   Figure 7 in Wang et al. (2014). As the TCCON N$_2$O retrievals are corrected to the WMO scale (Wunch et al., 2015) while HF retrievals has not been validated, the systematic bias is probably due to the uncertainty of the X_{HF} product. Second, at St Denis (a moist site), the TCCON HF retrievals are strongly affected by H$_2$O so that the TCCON proxy method tropospheric and the stratospheric X_{CH_4} data using HF have many outliers.

     Figure 9 also shows the time series of the tropospheric and stratospheric X_{CH_4} from the SFIT4NIR retrievals. The SFIT4NIR

10   tropospheric X_{CH_4} are close to the proxy data at St Denis, while the SFIT4NIR tropospheric X_{CH_4} are systematically larger than the results from the proxy method at the five sites located in the Northern Hemisphere. The vital difference between St Denis and other sites is that the tropopause height at St Denis is about 16.5 km, which is relatively higher than the tropopause height of 9-12 km at other sites. It seems that the partial column of CH$_4$ from the SFIT4NIR retrieval is larger than that from the TCCON proxy data in the vertical range from surface to about 10 km, while it is smaller than that from the TCCON proxy

15   data above 10 km. The bias in the in the vertical range from surface to 10 km might be able to get compensation from the part of 10 –16.5 km, due to the relatively high tropopause height at St Denis. The phases of the X_{CH_4} seasonal variations from the SFIT4NIR retrievals are almost the same as those from the proxy method, while the amplitudes of the variations from the SFIT4NIR retrievals are larger than those from the proxy method in the tropospheric component. There are 2 possible explanations: 1) the proxy method assumes that the vertical mole fraction profile of HF or N$_2$O are constant in the troposphere,

20   and the CH$_4$ mole fraction in the upper troposphere is calculated as the tropospheric X_{CH_4} for the proxy method; 2) the tropopause height in the proxy method has a chemical definition, which differs from the tropopause height calculated from the temperature and the altitude profiles (Wang et al., 2017).

3.5   AirCore measurements at Sodankylä

The AirCore is an atmospheric sampling system which uses a long tube to sample the air from the surrounding atmosphere

25   and preserve profiles of the trace gases of interest from the surface (few hundred meters) to the middle stratosphere (about 30 km) (Karion et al., 2010). Regular AirCore measurements of CH$_4$ have been carried out at Sodankylä since September 2013. During 2016-2017, we select 7 AirCore profiles which are within 1 hour of SFIT4NIR measurements.

     As an example, the AirCore CH$_4$ profile on 5 September 2017, together with the co-located (within $\pm$ 1 hour) SFIT4NIR a priori and retrieved profiles are shown in the left panel of Figure 10. AirCore and FTS data cannot be compared directly,

30   because the AirCore profile has a high vertical resolution but it covers only a part of the total column that is observed by the FTS. The AirCore measurement for this launch covers the vertical range from about 0.6 to 26 km, and needs to be extended to compare with the FTIR data. For the extrapolation, a scaled SFIT4NIR a priori profile is applied to extend the AirCore CH$_4$ profile above 26 km, and the local surface CH$_4$ mole fraction observations (Kilkki et al., 2015) are applied to extend the AirCore CH$_4$ profile below 0.6 km. In order to take the vertical sensitivity of the FTIR retrieval into account (Rodgers, 2003),
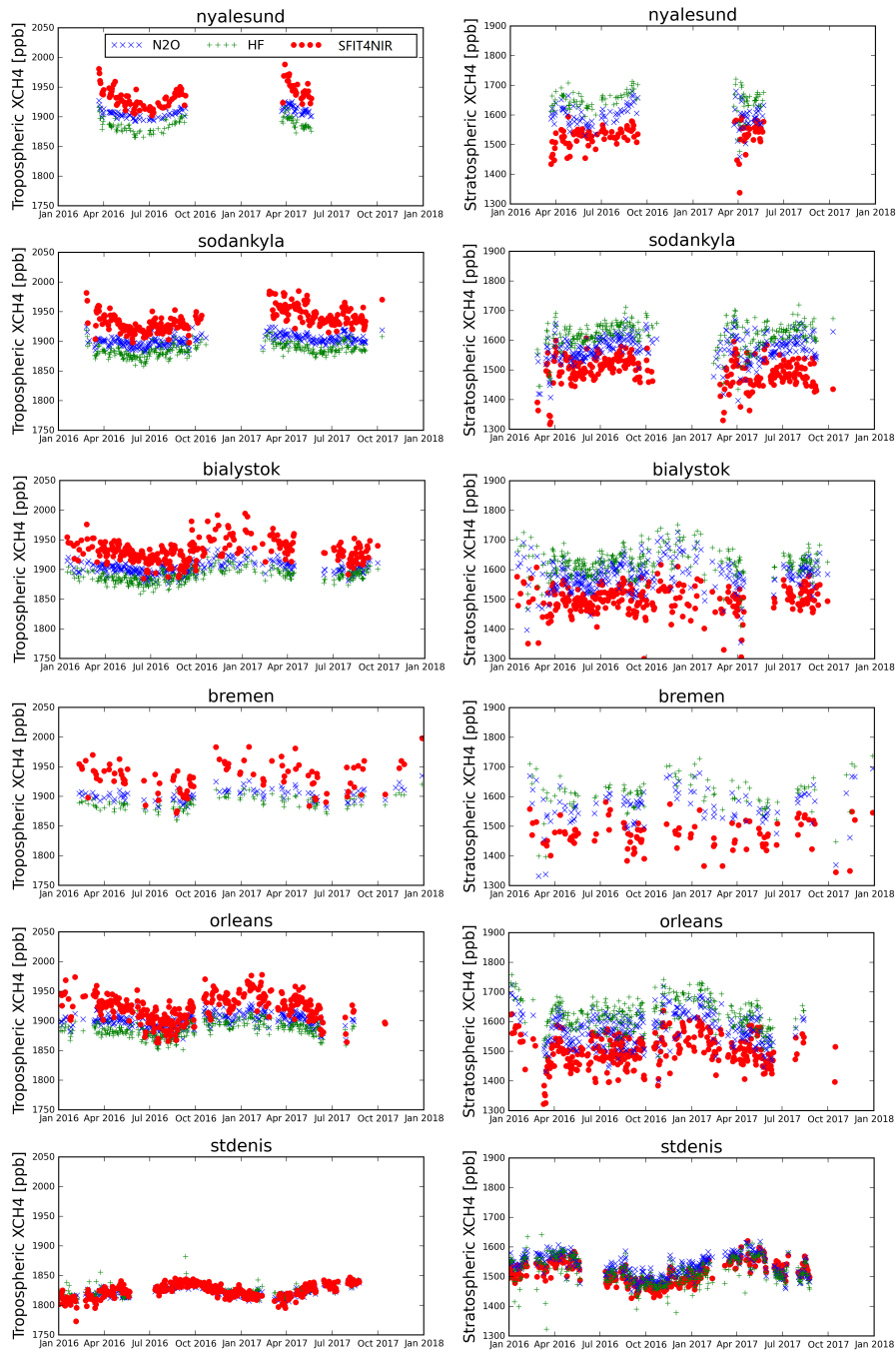
Figure 9. The time series of the tropospheric (left panels) and the stratospheric (right panels) co-located X_{CH_4} hourly means from the SFIT4NIR and the proxy method (both N_2O and HF) at the six TCCON sites.

the "extended" AirCore profile is then smoothed with the co-located SFIT4NIR retrieval

$$x_{aircore,s} = x_a + \mathbf{A}(x_{insitu} - x_a), \tag{9}$$

where x_{instu} is the "extended" AirCore profile, x_a is the a priori profile of the SFIT4NIR retrieval, and $x_{aircore,s}$ is the smoothed AirCore profile. The mean and the standard deviation of the relative differences between the co-located SFIT4NIR retrievals and the smoothed AirCore profile ((SFIT4NIR - AirCore) / AirCore $\times$ 100%) are shown in the right panel of Figure 10. The bias is about +1.5% in the lower and the middle troposphere, between +1 and -4% in the upper troposphere and lower stratosphere region, and about -2.5% in the middle and upper stratosphere.

Figure 11 shows the scatter plots of X_{CH_4} between the co-located SFIT4NIR retrievals and the AirCore measurements for the whole atmosphere, for the tropospheric and for the stratospheric components. The errorbars are the random uncertainties of the SFIT4NIR retrievals and the AirCore measurements. It is assumed that the random uncertainty of the AirCore profile is about 0.1% between the surface and its maximum measurement altitude ($\sim$ 30 km), and it is about 2% above the maximum measurement altitude. The slope of the regression line (a = 1.001) in the whole atmosphere indicates that there is almost no systematic difference between the SFIT4NIR and the AirCore X_{CH_4}, which is consistent with the result in the comparison between SFIT4NIR and TCCON X_{CH_4} measurements (Figures 5 and 6). The SFIT4NIR tropospheric X_{CH_4} is about 1.1 $\pm$ 0.4% larger than the AirCore measurements and the SFIT4NIR stratospheric X_{CH_4} is about 4.0 $\pm$ 2.0% less than the AirCore measurements. These differences between the SFIT4NIR retrievals and AirCore measurements are within the systematic uncertainties of the SFIT4NIR partial columns in the troposphere and stratosphere, and it is inferred that the systematic uncertainty of the SFIT4NIR partial column is mainly coming from the uncertainty of the spectroscopy (see Table 5).

3.6 Aircraft measurements during the IMECC campaign

The Infrastructure for Measurement of the European Carbon Cycle (IMECC) aircraft measurements passed over several European TCCON sites in September and October 2009, including Orléans, Bremen and Bialystok. We refer to Geibel et al. (2012) for a detail description of the IMECC aircraft data. The aircraft measurement covers a vertical range from about 300 to 13000 m, mainly in the troposphere. Therefore, in this section, we use the co-located aircraft measurements to compare with the SFIT4NIR tropospheric X_{CH_4}. The location, date and time of the overflight, SZA and the profile code are listed in the Table 1 in Geibel et al. (2012). There are 4 aircraft vertical profiles over Bialystok (BI-OF1a, BI-OF1b, BI-OF2a, BI-OF2b), 4 profiles over Orléans (OR-OF1a, OR-OF1b, OR-OF2a, OR-OF2b), and 2 profiles over Bremen (BR-OF1a, BR-OF2a).

To compare the aircraft measurements with the SFIT4NIR, the aircraft profile need to be extended to compare with FTIR retrievals. The extrapolation method is the same as described in Section 4.2 in Geibel et al. (2012). For the near-ground part, ground-based in-situ data from the co-located tall-tower stations are used to extend the aircraft data to the ground at Orléans and Bialystok, and the values measured at the lowermost altitude by the aircraft are linearly extrapolated to the surface at Bremen. For the upper part, the TCCON (GGG2012) a priori profile multiplied by the retrieval scaling factor is used. The uncertainties of "extended" aircraft profiles have been shown in Table 2 in Geibel et al. (2012). After that, the "extended" aircraft profile is smoothed with FTIR retrieval using Eq. 9, where the x_{insitu} is the aircraft measurement. The SFIT4NIR
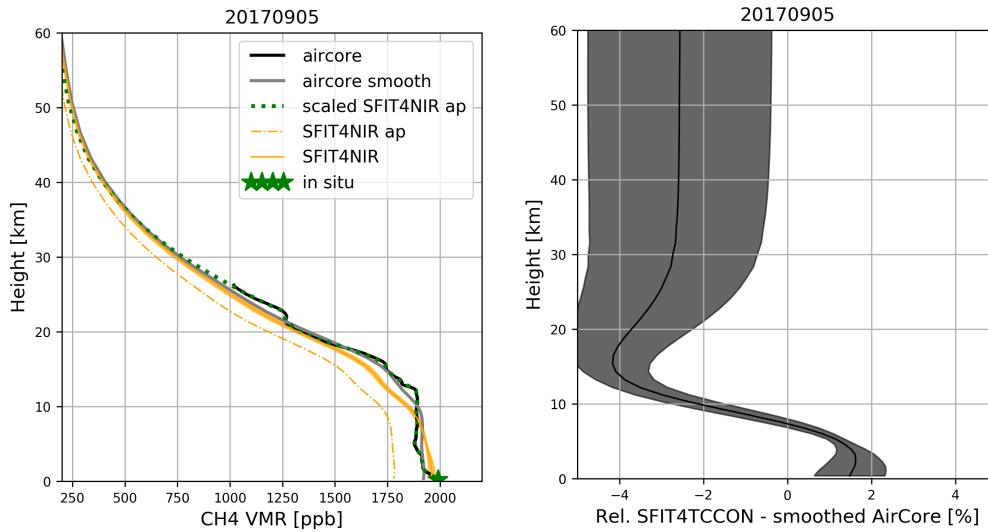
Figure 10. Left panel: the CH$_4$ profile from the AirCore measurement (solid black line) on 5 September 2017, together with the SFIT4NIR a priori (dash-dotted orange line) and retrieved (solid orange line) profiles. The AirCore measurement is extrapolated with the surface in situ measurements (green star) and the scaled SFIT4NIR a priori profile (dotted green line). The grey line is the smoothed AirCore profile. Right panel: the mean (solid black line) and the stand deviation (shadow) of relative difference between the co-located SFIT4NIR retrieved profiles and the smoothed AirCore measurements ((SFIT4NIR - AirCore) / AirCore × 100%).
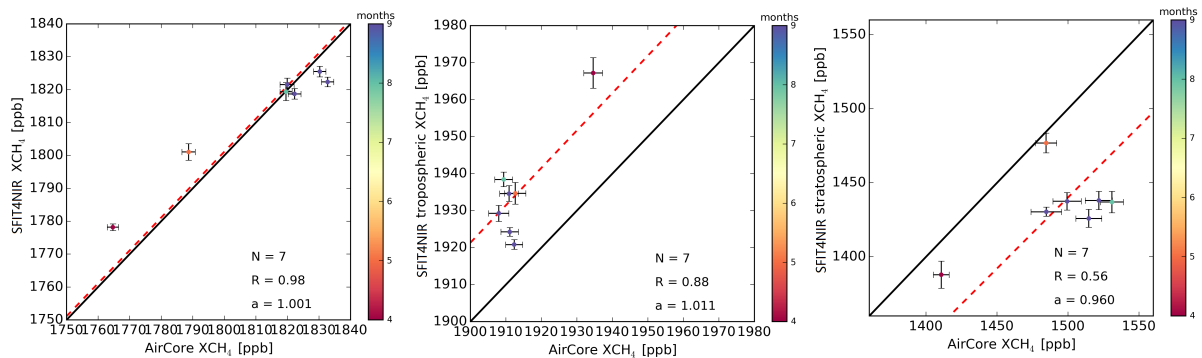
Figure 11. The scatter plots of X$_{CH_4}$ between the SFIT4NIR and the AirCore measurements for the whole atmosphere (left panel), for the tropospheric (middle panel) and for the stratospheric (right panel) components. In each panel, the black line is the one-to-one line and the dashed red line is the regression line with the intercept to zero ($y = a \cdot x$). N is the co-located measurement number, R is the correlation coefficient, and a is the slope.

retrievals within a time window of $\pm$ 1 hour around the aircraft overflight are chosen. The standard deviation of the co-located SFIT4NIR retrievals is used as the random uncertainty of the FTIR retrieval.

The smoothed aircraft tropospheric X_{CH_4} is 1.0 ± 0.2 % larger than the SFIT4NIR tropospheric X_{CH_4}, which is consistent with the result from the comparison between the AirCore measurements and SFIT4NIR retrievals (1.1 ± 0.4 %). Combining the AirCore measurements at Sodankylä and aircraft measurements at Orléans, Bremen and Bialystok, Figure 12 shows that there is a systematic overestimation of 1.0 ± 0.3 % in the SFIT4NIR tropospheric X_{CH_4}. Further investigation is required to see if the systematic bias can be observed at other sites.
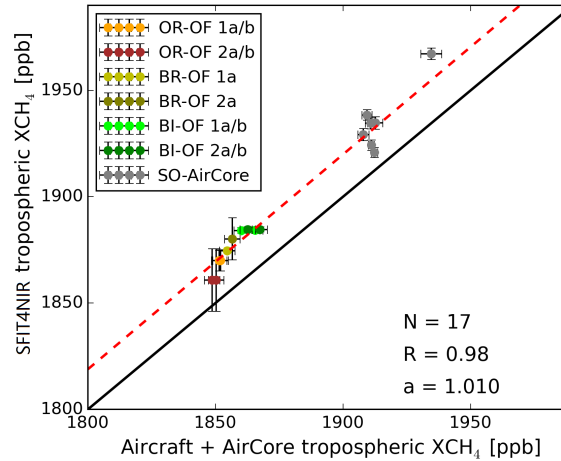
Figure 12. The scatter plots of X_{CH_4} between the SFIT4NIR and the IMECC aircraft measurements together with the AirCore measurements for the tropospheric components. The black line is the one-to-one line and the dashed red line is the regression line with the intercept to zero ($y = a \cdot x$). N is the co-located measurement number, R is the correlation coefficient, and a is the slope.

4 Conclusions

The retrieval of CH_4 vertical information from TCCON FTIR spectra has been carried out at six sites during 2016-2017 using the SFIT4 code. The retrieval strategy of the SFIT4NIR has been discussed, including the spectroscopy, retrieval window, a priori profile, SNR and regularization. The AVK shows that the SFIT4NIR retrieved profile is sensitive to the altitude range from the surface to the middle stratosphere (about 40 km), and the column averaging kernel has a good sensitivity in the whole atmosphere. The DOFS of the SFIT4NIR is about 2.4, with two distinct pieces of information in the troposphere and the stratosphere. The systematic and random uncertainties of the SFIT4NIR retrieved total column are about 3.2 and 0.5%.

The SFIT4NIR retrieved CH_4 total columns and partial columns (troposphere and stratosphere) have been evaluated based on the standard TCCON retrievals, ground-based in situ measurements, ACE-FTS satellite observations, TCCON proxy X_{CH_4} data, and AirCore measurements at Sodankylä. It is found that the SFIT4NIR retrieved X_{CH_4} data are very close to the standard TCCON retrievals with the mean bias between -0.14 and 0.15% and the standard deviation of bias between 0.3 and 0.5% at the six TCCON sites. Additionally, there is no obvious seasonal variation in the difference between the SFIT4NIR and TCCON

X_{CH_4} data. The SFIT4NIR tropospheric and stratospheric X_{CH_4} can observe the CH_4 seasonal variation very well, which has been confirmed by the ground-based in situ measurements and ACE-FTS observations, respectively. The tropospheric and the stratospheric X_{CH_4} from SFIT4NIR retrievals have also been compared with the results from the TCCON proxy method. The phases of the seasonal cycles from SFIT4NIR retrievals and TCCON proxy data are consistent, though the amplitudes of the variations from the SFIT4NIR retrievals are relatively larger than those from the proxy method, especially in the troposphere. Further investigation is needed to understand the accuracy of the seasonal cycle from the SFIT4NIR tropospheric X_{CH_4} when more aircraft or AirCore measurements become available. By comparison against AirCore measurements at Sodankylä, it is found that there is almost no systematic bias between the SFIT4NIR and AirCore X_{CH_4} (in the whole atmosphere), which is consistent with the comparison between the SFIT4NIR and the TCCON standard retrievals. An underestimation of $4.0 \pm 2.0\%$ in the SFIT4NIR stratospheric X_{CH_4} is seen by comparing with AirCore measurements, and an overestimation of $1.0 \pm 0.3\%$ in the SFIT4NIR tropospheric X_{CH_4} is seen by comparing with AirCore measurements and IMECC aircraft measurements. These biases are within the systematic uncertainties of SFIT4NIR retrieved partial columns in the troposphere and stratosphere, respectively.

References

Agusti-Panareda, A., Diamantakis, M., Bayona, V., Klappenbach, F., and Butz, A.: Improving the inter-hemispheric gradient of total column atmospheric CO2and CH4 in simulations with the ECMWF semi-Lagrangian atmospheric global model, Geosci. Model Dev., 10, 1–18, https://doi.org/10.5194/gmd-10-1-2017, 2017.

5 Bernath, P. F., McElroy, C. T., Abrams, M. C., Boone, C. D., Butler, M., Camy-Peyret, C., Carleer, M., Clerbaux, C., Coheur, P. F., Colin, R., DeCola, P., DeMazière, M., Drummond, J. R., Dufour, D., Evans, W. F. J., Fast, H., Fussen, D., Gilbert, K., Jennings, D. E., Llewellyn, E. J., Lowe, R. P., Mahieu, E., McConnell, J. C., McHugh, M., McLeod, S. D., Michaud, R., Midwinter, C., Nassar, R., Nichitiu, F., Nowlan, C., Rinsland, C. P., Rochon, Y. J., Rowlands, N., Semeniuk, K., Simon, P., Skelton, R., Sloan, J. J., Soucy, M. A., Strong, K., Tremblay, P., Turnbull, D., Walker, K. A., Walkty, I., Wardle, D. A., Wehrle, V., Zander, R., and Zou, J.: Atmospheric chemistry experiment
10 (ACE): Mission overview, Geophys. Res. Lett., 32, https://doi.org/10.1029/2005GL022386, 2005.

De Maziere, M., Vigouroux, C., Bernath, P. F., Baron, P., Blumenstock, T., Boone, C., Brogniez, C., Catoire, V., Coffey, M., Duchatelet, P., Griffith, D., Hannigan, J., Kasai, Y., Kramer, I., Jones, N. B., Mahieu, E., Manney, G. L., Piccolo, C., Randall, C., Robert, C., Senten, C., Strong, K., Taylor, J., Tetard, C., Walker, K. a., and Wood, S.: Validation of ACE-FTS v2.2 methane profiles from the upper troposphere to the lower mesosphere, Atmos. Chem. Phys, 8, 2421–2435, https://doi.org/10.5194/acp-8-2421-2008, 2008.

15 De Mazière, M., Sha, M. K., Desmet, F., Hermans, C., Scolas, F., Kumps, N., Metzger, J.-M., Duflot, V., and Cammas, J.-P.: TCCON data from Reunion Island (RE), Release GGG2014R0, TCCON data archive, hosted by CaltechDATA, https://doi.org/10.14291/tccon.ggg2014.reunion01.R0/1149288, 2014.

De Mazière, M., Thompson, A. M., Kurylo, M. J., Wild, J. D., Bernhard, G., Blumenstock, T., Braathen, G. O., Hannigan, J. W., Lambert, J.-C., Leblanc, T., McGee, T. J., Nedoluha, G., Petropavlovskikh, I., Seckmeyer, G., Simon, P. C., Steinbrecht, W., and Strahan, S. E.:
20 The Network for the Detection of Atmospheric Composition Change (NDACC): history, status and perspectives, Atmos. Chem. Phys., 18, 4935–4964, https://doi.org/10.5194/acp-18-4935-2018, 2018.

Deutscher, N. M., Griffith, D. W., Bryant, G. W., Wennberg, P. O., Toon, G. C., Washenfelder, R. A., Keppel-Aleks, G., Wunch, D., Yavin, Y., Allen, N. T., Blavier, J. F., Jiménez, R., Daube, B. C., Bright, A. V., Matross, D. M., Wofsy, S. C., and Park, S.: Total column CO2measurements at Darwin, Australia - Site description and calibration against in situ aircraft profiles, Atmos. Meas. Tech., 3, 947–958,
25 https://doi.org/10.5194/amt-3-947-2010, 2010.

Deutscher, N. M., Notholt, J., Messerschmidt, J., Weinzierl, C., Warneke, T., Petri, C., Grupe, P., and Katrynski, K.: TCCON data from Bialystok (PL), Release GGG2014R0, TCCON data archive, hosted by CaltechDATA, https://doi.org/10.14291/tccon.ggg2014.bialystok01.R0/1149277, 2014.

Dils, B., Buchwitz, M., Reuter, M., Schneising, O., Boesch, H., Parker, R., Guerlet, S., Aben, I., Blumenstock, T., Burrows, J. P., Butz, A.,
30 Deutscher, N. M., Frankenberg, C., Hase, F., Hasekamp, O. P., Heymann, J., De Mazière, M., Notholt, J., Sussmann, R., Warneke, T., Griffith, D., Sherlock, V., and Wunch, D.: The greenhouse gas climate change initiative (GHG-CCI): Comparative validation of GHG-CCI SCIAMACHY/ENVISAT and TANSO-FTS/GOSAT CO2 and CH4 retrieval algorithm products with measurements from the TCCON, Atmos. Meas. Tech., 7, 1723–1744, https://doi.org/10.5194/amt-7-1723-2014, 2014.

Ehhalt, D. H. and Heidt, L. E.: Vertical profiles of CH4 in the troposphere and stratosphere, J. Geophys. Res., 78, 5265–5271,
35 https://doi.org/10.1029/JC078i024p05265, 1973.

European Commission, .: Emission Database for Global Atmospheric Research (EDGAR), release EDGARv4.2 FT2010, Tech. rep., Joint Research Centre (JRC)/Netherlands Environmental Assessment Agency (PBL). last access: 12 April 2018, http://edgar.jrc.ec.europa.eu, 2013.

Fraser, A., Palmer, P. I., Feng, L., Boesch, H., Cogan, A., Parker, R., Dlugokencky, E. J., Fraser, P. J., Krummel, P. B., Langenfelds, R. L.,
O'Doherty, S., Prinn, R. G., Steele, L. P., Van Der Schoot, M., and Weiss, R. F.: Estimating regional methane surface fluxes: The relative importance of surface and GOSAT mole fraction measurements, Atmos. Chem. Phys., 13, 5697–5713, https://doi.org/10.5194/acp-13-5697-2013, 2013.

Geibel, M. C., Messerschmidt, J., Gerbig, C., Blumenstock, T., Chen, H., Hase, F., Kolle, O., Lavrič, J. V., Notholt, J., Palm, M., Rettinger,
M., Schmidt, M., Sussmann, R., Warneke, T., and Feist, D. G.: Calibration of column-averaged CH_4 over European TCCON FTS sites
with airborne in-situ measurements, Atmos. Chem. Phys., 12, 8763–8775, https://doi.org/10.5194/acp-12-8763-2012, 2012.

Houweling, S., Krol, M., Bergamaschi, P., Frankenberg, C., Dlugokencky, E. J., Morino, I., Notholt, J., Sherlock, V., Wunch, D., Beck,
V., Gerbig, C., Chen, H., Kort, E. A., Röckmann, T., and Aben, I.: A multi-year methane inversion using SCIAMACHY, accounting for systematic errors using TCCON measurements, Atmos. Chem. Phys., 14, 3991–4012, https://doi.org/10.5194/acp-14-3991-2014, 2014.

IPCC: Climate change 2013: The physical science basis. Contribution of Working Group I to the Fifth Assessment Report of the Intergovernmental Panel on Climate Change, 2013.

Karion, A., Sweeney, C., Tans, P., and Newberger, T.: AirCore: An innovative atmospheric sampling system, J. Atmos. Ocean. Technol., 27,
1839–1853, https://doi.org/10.1175/2010JTECHA1448.1, 2010.

Keppel-Aleks, G., Toon, G. C., Wennberg, P. O., and Deutscher, N. M.: Reducing the impact of source brightness fluctuations on spectra
obtained by Fourier-transform spectrometry., Appl. Opt., 46, 4774–4779, https://doi.org/10.1364/AO.46.004774, 2007.

Kilkki, J., Aalto, T., Hatakka, J., Portin, H., and Laurila, T.: Atmospheric CO2 observations at Finnish urban and rural sites, Boreal Environ.
Res., 20, 227–242, 2015.

Kirschke, S., Bousquet, P., Ciais, P., Saunois, M., Canadell, J. G., Dlugokencky, E. J., Bergamaschi, P., Bergmann, D., Blake, D. R., Bruhwiler,
L., Cameron-Smith, P., Castaldi, S., Chevallier, F., Feng, L., Fraser, A., Heimann, M., Hodson, E. L., Houweling, S., Josse, B., Fraser, P. J.,
Krummel, P. B., Lamarque, J.-F., Langenfelds, R. L., Le Quéré, C., Naik, V., O'Doherty, S., Palmer, P. I., Pison, I., Plummer, D., Poulter,
B., Prinn, R. G., Rigby, M., Ringeval, B., Santini, M., Schmidt, M., Shindell, D. T., Simpson, I. J., Spahni, R., Steele, L. P., Strode, S. A.,
Sudo, K., Szopa, S., van der Werf, G. R., Voulgarakis, A., van Weele, M., Weiss, R. F., Williams, J. E., and Zeng, G.: Three decades of
global methane sources and sinks, Nat. Geosci., https://doi.org/10.1038/ngeo1955, 2013.

Kivi, R., Heikkinen, P., and Kyrö, E.: TCCON data from Sodankyla (FI), Release GGG2014R0, TCCON data archive, hosted by Caltech-DATA, https://doi.org/10.14291/tccon.ggg2014.sodankyla01.R0/1149280, 2014.

Notholt, J., Petri, C., Warneke, T., Deutscher, N. M., Buschmann, M., Weinzierl, C., Macatangay, R., and Grupe,
P.: TCCON data from Bremen (DE), Release GGG2014R0, TCCON data archive, hosted by CaltechDATA,
https://doi.org/10.14291/tccon.ggg2014.bremen01.R0/1149275, 2014.

Notholt, J., Warneke, T., Petri, C., Deutscher, N. M., Weinzierl, C., Palm, M., and Buschmann, M.: TCCON
data from Ny Ålesund, Spitsbergen (NO), Release GGG2014.R0, TCCON data archive, hosted by CaltechDATA,
https://doi.org/10.14291/tccon.ggg2014.nyalesund01.R0/1149278, 2017.

Ostler, A., Sussmann, R., Patra, P. K., Houweling, S., De Bruine, M., Stiller, G. P., Haenel, F. J., Plieninger, J., Bousquet, P., Yin, Y., Saunois,
M., Walker, K. A., Deutscher, N. M., Griffith, D. W. T., Blumenstock, T., Hase, F., Warneke, T., Wang, Z., Kivi, R., and Robinson, J.:

Evaluation of column-averaged methane in models and TCCON with a focus on the stratosphere, Atmos. Meas. Tech., 9, 4843–4859, https://doi.org/10.5194/amt-9-4843-2016, 2016.

Pougatchev, N. S., Connor, B. J., and Rinsland, C. P.: Infrared measurements of the ozone vertical distribution above Kitt Peak, J. Geophys. Res., 100, 16 689, https://doi.org/10.1029/95JD01296, 1995.

5   Rigby, M., Prinn, R. G., Fraser, P. J., Simmonds, P. G., Langenfelds, R. L., Huang, J., Cunnold, D. M., Steele, L. P., Krummel, P. B., Weiss, R. F., O'Doherty, S., Salameh, P. K., Wang, H. J., Harth, C. M., Mühle, J., and Porter, L. W.: Renewed growth of atmospheric methane, Geophys. Res. Lett., 35, L22 805, https://doi.org/10.1029/2008GL036037, 2008.

Rodgers, C. D.: Inverse Methods for Atmospheric Sounding – Theory and Practice, Series on Atmospheric Oceanic and Planetary Physics, vol. 2, World Scientific Publishing Co. Pte. Ltd, Singapore, https://doi.org/10.1142/9789812813718, 2000.

10   Rodgers, C. D.: Intercomparison of remote sounding instruments, J. Geophys. Res., 108, 46–48, https://doi.org/10.1029/2002JD002299, 2003.

Rothman, L. S., Gordon, I. E., Babikov, Y., Barbe, A., Chris Benner, D., Bernath, P. F., Birk, M., Bizzocchi, L., Boudon, V., Brown, L. R., Campargue, A., Chance, K., Cohen, E. A., Coudert, L. H., Devi, V. M., Drouin, B. J., Fayt, A., Flaud, J. M., Gamache, R. R., Harrison, J. J., Hartmann, J. M., Hill, C., Hodges, J. T., Jacquemart, D., Jolly, A., Lamouroux, J., Le Roy, R. J., Li, G., Long, D. A.,

15   Lyulin, O. M., Mackie, C. J., Massie, S. T., Mikhailenko, S., Müller, H. S. P., Naumenko, O. V., Nikitin, A. V., Orphal, J., Perevalov, V., Perrin, A., Polovtseva, E. R., Richard, C., Smith, M. A. H., Starikova, E., Sung, K., Tashkun, S., Tennyson, J., Toon, G. C., Tyuterev, V. G., and Wagner, G.: The HITRAN2012 molecular spectroscopic database, J. Quant. Spectrosc. Radiat. Transf., 130, 4–50, https://doi.org/10.1016/j.jqsrt.2013.07.002, 2013.

Saad, K. M., Wunch, D., Toon, G. C., Bernath, P., Boone, C., Connor, B., Deutscher, N. M., Griffith, D. W. T., Kivi, R., Notholt, J.,

20   Roehl, C., Schneider, M., Sherlock, V., and Wennberg, P. O.: Derivation of tropospheric methane from TCCON CH_4 and HF total column observations, Atmos. Meas. Tech., 7, 2907–2918, https://doi.org/10.5194/amt-7-2907-2014, 2014.

Saad, K. M., Wunch, D., Deutscher, N. M., Griffith, D. W., Hase, F., De Mazière, M., Notholt, J., Pollard, D. F., Roehl, C. M., Schneider, M., Sussmann, R., Warneke, T., and Wennberg, P. O.: Seasonal variability of stratospheric methane: Implications for constraining tropospheric methane budgets using total column observations, Atmos. Chem. Phys., 16, 14 003–14 024, https://doi.org/10.5194/acp-16-14003-2016,

25   2016.

Saito, R., Patra, P. K., Deutscher, N., Wunch, D., Ishijima, K., Sherlock, V., Blumenstock, T., Dohe, S., Griffith, D., Hase, F., Heikkinen, P., Kyrö, E., MacAtangay, R., Mendonca, J., Messerschmidt, J., Morino, I., Notholt, J., Rettinger, M., Strong, K., Sussmann, R., and Warneke, T.: Technical Note: Latitude-time variations of atmospheric column-average dry air mole fractions of CO_2, CH_4 and N_2O, Atmos. Chem. Phys., 12, 7767–7777, https://doi.org/10.5194/acp-12-7767-2012, 2012.

30   Schmidt, M., Lopez, M., Yver Kwok, C., Messager, C., Ramonet, M., Wastine, B., Vuillemin, C., Truong, F., Gal, B., Parmentier, E., Cloué, O., and Ciais, P.: High-precision quasi-continuous atmospheric greenhouse gas measurements at Trainou tower (Orléans forest, France), Atmos. Meas. Tech., 7, 2283–2296, https://doi.org/10.5194/amt-7-2283-2014, 2014.

Sheese, P. E., Boone, C. D., and Walker, K. A.: Detecting physically unrealistic outliers in ACE-FTS atmospheric measurements, Atmos. Meas. Tech., 8, 741–750, https://doi.org/10.5194/amt-8-741-2015, 2015.

35   Tikhonov, A. N.: Solution of Incorrectly Formulated Problems and the Regularisation Method, Soviet. Math. Dokl., 4, 1035–1038, https://doi.org/10.1111/J.1365-246X.2012.05699.X, 1963.

Toon, G. C.: Telluric line list for GGG2014, TCCON data archive, hosted by the Carbon Dioxide Information Analysis Center, Oak Ridge National Laboratory, Oak Ridge, Tennessee, U.S.A., https://doi.org/10.14291/tccon.ggg2014.atm.R0/1221656, 2014.

Tukiainen, S., Railo, J., Laine, M., Hakkarainen, J., Kivi, R., Heikkinen, P., Chen, H., and Tamminen, J.: Retrieval of atmospheric CH4 profiles from Fourier transform infrared data using dimension reduction and MCMC, J. Geophys. Res. Atmos., 121, 10,312–10,327, https://doi.org/10.1002/2015JD024657, https://agupubs.onlinelibrary.wiley.com/doi/abs/10.1002/2015JD024657, 2016.

Wang, Z., Deutscher, N. M., Warneke, T., Notholt, J., Dils, B., Griffith, D. W. T., Schmidt, M., Ramonet, M., and Gerbig, C.: Retrieval of tropospheric column-averaged CH4 mole fraction by solar absorption FTIR-spectrometry using N2O as a proxy, Atmos. Meas. Tech., 7, 3295–3305, https://doi.org/10.5194/amt-7-3295-2014, 2014.

Wang, Z., Warneke, T., Deutscher, N. M., Notholt, J., Karstens, U., Saunois, M., Schneider, M., Sussmann, R., Sembhi, H., Griffith, D. W. T., Pollard, D. F., Kivi, R., Petri, C., Velazco, V. A., Ramonet, M., and Chen, H.: Contributions of the troposphere and stratosphere to CH4 model biases, Atmos. Chem. Phys., 17, 13 283–13 295, https://doi.org/10.5194/acp-17-13283-2017, 2017.

Warneke, T., Messerschmidt, J., Notholt, J., Weinzierl, C., Deutscher, N. M., Petri, C., Grupe, P., Vuillemin, C., Truong, F., Schmidt, M., Ramonet, M., and Parmentier, E.: TCCON data from Orléans (FR), Release GGG2014R0, TCCON data archive, hosted by CaltechDATA, https://doi.org/10.14291/tccon.ggg2014.orleans01.R0/1149276, 2014.

Waymark, C., Waymark, C., Walker, K., Boone, C. D., and Bernath, P. F.: ACE-FTS version 3.0 data set: validation and data processing update, Ann. Geophys., 56, https://doi.org/10.4401/ag-6339, 2014.

Wunch, D., Toon, G. C., Blavier, J.-F. L., Washenfelder, R. A., Notholt, J., Connor, B. J., Griffith, D. W. T., Sherlock, V., and Wennberg, P. O.: The Total Carbon Column Observing Network, Philos. Trans. R. Soc. A Math. Phys. Eng. Sci., 369, 2087–2112, https://doi.org/10.1098/rsta.2010.0240, 2011.

Wunch, D., Toon, G. C., Sherlock, V., Deutscher, N. M., Liu, C., Feist, D. G., and Wennberg, P. O.: The Total Carbon Column Observing Network's GGG2014 Data Version, p. 43, http://dx.doi.org/10.14291/tccon.ggg2014.documentation.R0/1221662, 2015.

Wunch, D., Toon, G. C., Hedelius, J. K., Vizenor, N., Roehl, C. M., Saad, K. M., Blavier, J. F. L., Blake, D. R., and Wennberg, P. O.: Quantifying the loss of processed natural gas within California's South Coast Air Basin using long-term measurements of ethane and methane, Atmos. Chem. Phys., 16, 14 091–14 105, https://doi.org/10.5194/acp-16-14091-2016, 2016.

Yang, Z., Toon, G. C., Margolis, J. S., and Wennberg, P. O.: Atmospheric CO2 retrieved from ground-based near IR solar spectra, Geophys. Res. Lett., 29, 53–1–53–4, https://doi.org/10.1029/2001GL014537, 2002.

Zhou, M., Dils, B., Wang, P., Detmers, R., Yoshida, Y., O'Dell, C. W., Feist, D. G., Velazco, V. A., Schneider, M., and De Mazière, M.: Validation of TANSO-FTS/GOSAT XCO2 and XCH4 glint mode retrievals using TCCON data from near-ocean sites, Atmos. Meas. Tech., 9, 1415–1430, https://doi.org/10.5194/amt-9-1415-2016, 2016.

Zhou, M., Langerock, B., Vigouroux, C., Sha, M. K., Ramonet, M., Delmotte, M., Mahieu, E., Bader, W., Hermans, C., Kumps, N., Metzger, J.-M., Duflot, V., Wang, Z., Palm, M., and De Mazière, M.: Atmospheric CO and CH4 time series and seasonal variations on Reunion Island from ground-based in-situ and FTIR (NDACC and TCCON) measurements, Atmos. Chem. Phys., 18, 13 881–13 901, https://doi.org/10.5194/acp-18-13881-2018, 2018.